ROZPRAWY INŻYNIERSKIE • ENGINEERING TRANSACTIONS • 23, 2, 263—273, 1975
Polska Akademia Nauk • Instytut Podstawowych Problemów Techniki

QUASI-STATIC THERMAL STRESSES IN AN INFINITE SLAB

K. SAKAINO AND A. ATSUMI (SENDAI)

This paper deals with two thermoelastic problems of an infinite slab with or without a cylindrical hole. The thermal stress distribution which arises in a slab if a circular region of the plane boundary (Case A), or a cylindrical boundary (Case B) undergoes a sudden temperature change, is analysed using a thermoelastic potential and a stress function. In both cases, it is considered and graphically shown how the ratio of the radius of the heated circular region, or cylindrical hole, to the plate thickness affects the thermal stress distribution.

NOTATION

a radius of circular region in Case A, of the cylindrical hole in Case B,
d plate thickness,
r, z cylindrical coordinates,
$\nabla^2 = \frac{\partial^2}{\partial r^2} + \frac{1}{r}\frac{\partial}{\partial r} + \frac{\partial^2}{\partial z^2}$ Laplacian operator,
T temperature,
κ thermal diffusivity,
t time,
T_0 constant temperature,
$J_n(\ )$ Bessel function of the first kind in order n,
$Y_n(\ )$ Bessel function of the second kind in order n,
Φ thermoelastic potential,
ν Poisson's ratio,
α coeffiicient of linear thermal expansion,
E Young's modulus,
σ_r radial stress,
σ_θ circumferential stress,
σ_r axial stress,
τ_{rz} shear stress,
ψ, χ stress function,
u, w component of the displacement vector in r- and z-directions,
$K_n(\ )$ modified Bessel function of the second kind in order n.

1. Introduction

When the surfaces of machine elements are partially heated in casting, welding works etc, thermal stresses arise in them, which may often cause the structure breaks. Therefore, it is very significant to clarify the temperature field and the thermal stress distributions in the slab. Such thermoelastic problems have been investigated many times before. For example, Heisler [1] has studied the infinite slab which is exposed to an instantaneous uniform change in temperature, and Muki [2] has treated the steady thermoelasticity of a slab whose surface is partially heated, and Koizumi [3] has dealt with the quasi-static case that slab with a circular hole is uniformly heated.

The present investigation concerns two cases of quasi-static problems. In the first problem (Case A), the circular regions of the upper and lower surfaces are heated. The second problem (Case B) is that of an infinite slab with a cylindrical hole only whose surface is heated. In both cases, the initial temperature is zero everywhere, and the circular region (Case A) or the cylindrical hole (Case B) undergoes a sudden temperature change. The problems are analysed using a thermoelastic potential and a stress function. Numerical calculations are carried out for each case, and it is considered and graphically shown how the plate thickness affects the thermal stress distributions.

Numerical results will be of use of engineers and designers.

2. Solution of the equation of heat conduction

The coordinate system is shown in Fig. 1. The material is supposed to be homogeneous and isotropic with respect to both its thermal and mechanical response, and all physical properties are regarded as independent of temperature. Furthermore, the treatment is quasi-static in the conventional sense that inertia effects are neglected along with the absence of internal heat sources, which are required to obey the equation of Fourier's heat conduction in the form

$$\nabla^2 T=\frac{1}{\kappa}\frac{\partial T}{\partial t}. \tag{2.1}$$

At this stage it is expedient to introduce the dimensionless variables

$$\rho=\frac{r}{d},\quad \rho_1=\frac{a}{d},\quad \zeta=\frac{z}{d},\quad \omega_n=\frac{(2n+1)}{2}\pi,\quad \tau=\frac{\kappa t}{d^2}. \tag{2.2}$$

The initial condition and the boundary conditions are given for each case as follows:

for Case A

$$[T]_{\tau=0}=0,$$
$$[T]_{\zeta=\pm 1}=T_0\rho_1\int_0^\infty J_1(\xi\rho_1)J_0(\xi\rho)\,d\xi,\quad \tau>0; \tag{2.3}$$

for Case B

$$\left.\begin{aligned} &[T]_{\tau=0}=0,\\ &[T]_{\zeta=\pm 1}=0,\\ &[T]_{\rho=\rho_1}=T_0\sum_{n=0}^{\infty} a_n\cos\omega_n\zeta \end{aligned}\right\}, \qquad \tau>0. \tag{2.4}$$

Now, in the consideration of the initial and boundary conditions, the Laplace transform and the Hankel transform [4] are introduced to solve the Eq. (2.1) for Case A. For Case B, we use the Laplace transform and the method of variable

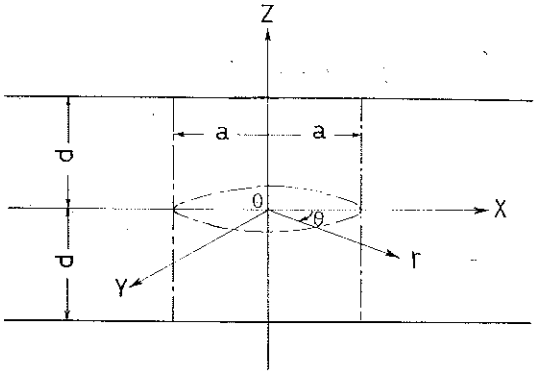

Fig. 1. Coordinate system.

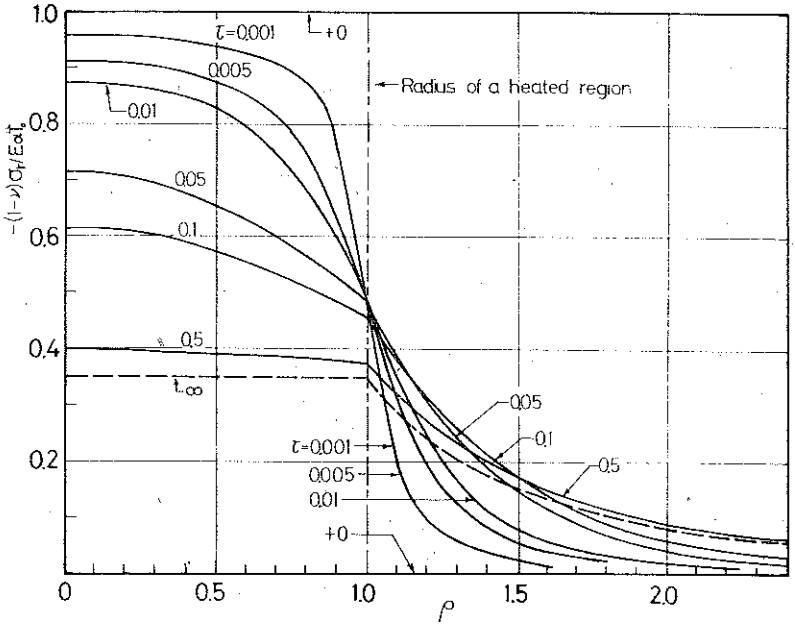

Fig. 2. Radial stresses on the surface of a slab.

separation. Performing the inverse integrals, we obtain each temperature solution as follows:

for case A

$$\frac{T}{T_0}=\rho_1\int_0^\infty \frac{\mathrm{ch}}{\mathrm{ch}}\frac{\xi\zeta}{\xi}J_1(\xi\rho_1)J_0(\xi\rho)\,d\xi+ \tag{2.5}$$

$$+2\rho_1\sum_{n=0}^{\infty}(-1)^{n+1}\omega_n\cos\omega_n\zeta\int_0^\infty\frac{e^{-\tau(\xi^2+\omega_n^2)}}{(\xi^2+\omega_n^2)}J_1(\xi\rho_1)J_0(\xi\rho)\,d\xi,$$

for case B

$$\frac{T}{T_0}=\sum_{n=0}^{\infty}a_n\cos\omega_n\zeta\left[\frac{K_0(\omega_n\rho)}{K_0(\omega_n\rho_1)}+\right. \tag{2.6}$$

$$\left.+\frac{2}{\pi}\int_0^\infty\frac{\xi e^{-\tau(\xi^2+\omega_n^2)}}{(\xi^2+\omega_n^2)}\,\frac{J_0(\xi\rho)\,Y_0(\xi\rho_1)-Y_0(\xi\rho)J_0(\xi\rho_1)}{J_0^2(\xi\rho_1)+Y_0^2(\xi\rho_1)}\,d\xi\right].$$

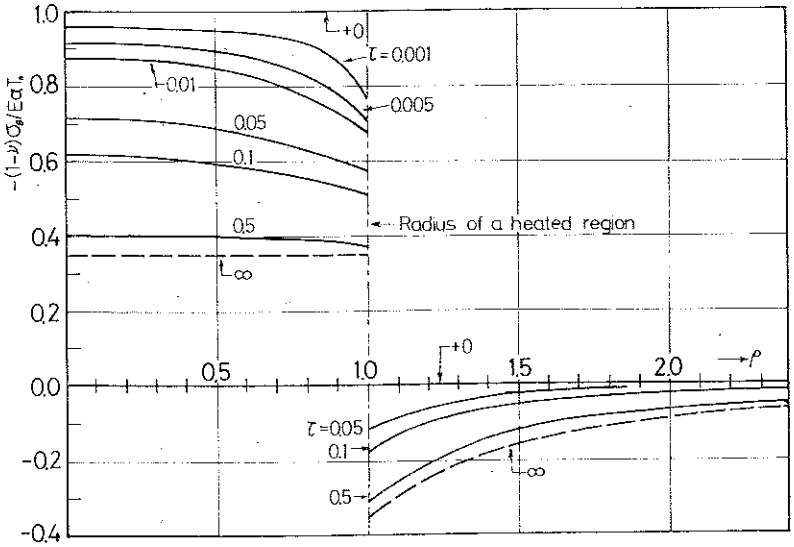

Fig. 3. Circumferential stresses on the surface of a slab.

3. Potential of thermoelastic displacement

To find the state of stress, we shall use the potential of thermoelastic displacement Φ, which is the particular solution of Poisson's equation [5]

$$\nabla^2\Phi=\frac{1+\nu}{1-\nu}\alpha T. \tag{3.1}$$

The stress field corresponding to the function Φ is easily found to be

$$\sigma_r^{(1)}=\frac{E}{1+\nu}\left(\frac{\partial^2\Phi}{\partial r^2}-\nabla^2\Phi\right),\qquad \sigma_\theta^{(1)}=\frac{E}{1+\nu}\left(\frac{1}{r}\frac{\partial\Phi}{\partial r}-\nabla^2\Phi\right),$$

$$\sigma_z^{(1)}=\frac{E}{1+\nu}\left(\frac{\partial^2\Phi}{\partial z^2}-\nabla^2\Phi\right),\qquad \tau_{rz}^{(1)}=\frac{E}{1+\nu}\frac{\partial^2\Phi}{\partial r\,\partial z}. \tag{3.2}$$

The particular solution of the Eq. (3.1) is given as follows:

for case A

$$\frac{1-\nu}{1+\nu}\frac{\Phi}{\alpha T_0 d^2}=\frac{\rho_1}{2}\int_0^\infty\frac{\zeta\,\mathrm{sh}\,\xi\zeta}{\xi\,\mathrm{ch}\,\xi}J_1(\xi\rho_1)J_0(\xi\rho)\,d\xi+$$
$$+2\rho_1\sum_{n=0}^{\infty}(-1)^n\omega_n\cos\omega_n\zeta\int_0^\infty\frac{e^{-\tau(\xi^2+\omega_n^2)}}{(\xi^2+\omega_n^2)^2}J_1(\xi\rho_1)J_0(\xi\rho)\,d\xi, \tag{3.3}$$

for case B

$$\frac{1-\nu}{1+\nu}\frac{\Phi}{\alpha T_0 d^2}=-\frac{1}{2}\sum_{n=0}^{\infty}a_n\cos\omega_n\zeta\left[\frac{\rho K_1(\omega_n\rho)}{\omega_n K_0(\omega_n\rho_1)}+\right.$$
$$\left.+\frac{4}{\pi}\int_0^\infty\frac{\xi e^{-\tau(\xi^2+\omega_n^2)}}{(\xi^2+\omega_n^2)^2}C_0(\xi\rho)\,d\xi\right], \tag{3.4}$$

where

$$C_n(\xi\rho)=\frac{Y_0(\xi\rho_1)J_n(\xi\rho)-J_0(\xi\rho_1)\,Y_n(\xi\rho)}{J_0^2(\xi\rho_1)+Y_0^2(\xi\rho_1)}.$$

4. Stress function

It can be seen that the stress does not satisfy the boundary conditions on the surfaces of the slab, as well as on the cylindrical surface of the hole in Case B, where tractions should vanish. In order to complete the boundary conditions, we make use of the stress functions [5, 6], which are defined as follows:

for Case A

$$\sigma_r^{(2)}=\frac{E}{1+\nu}\left\{\frac{\partial^2\psi_1}{\partial r^2}+z\frac{\partial^2\psi_2}{\partial r^2}-2\nu\frac{\partial\psi_2}{\partial z}\right\},$$

$$\sigma_\theta^{(2)}=\frac{E}{1+\nu}\left\{\frac{1}{r}\frac{\partial\psi_1}{\partial r}+\frac{z}{r}\frac{\partial\psi_2}{\partial r}-2\nu\frac{\partial\psi_2}{\partial z}\right\},$$

$$\sigma_z^{(2)}=\frac{E}{1+\nu}\left\{\frac{\partial^2\psi_1}{\partial z^2}+z\frac{\partial^2\psi_2}{\partial z^2}-2(1-\nu)\frac{\partial\psi_2}{\partial z}\right\}, \tag{4.1}$$

$$\tau_{rz}^{(2)}=\frac{E}{1+\nu}\left\{\frac{\partial^2\psi_1}{\partial r\,\partial z}+z\frac{\partial^2\psi_2}{\partial r\,\partial z}-(1-2\nu)\frac{\partial\psi_2}{\partial r}\right\},$$

where $\nabla^2\psi_1=\nabla^2\psi_2=0$.

for Case B

$$\sigma_r^{(2)}=\frac{E}{1+\nu}\left\{\frac{\partial^2\chi_1}{\partial r^2}+z\frac{\partial^2\chi_2}{\partial r^2}-2\nu\frac{\partial\chi_2}{\partial z}+r\frac{\partial^2\chi_3}{\partial r\,\partial z}+(1-2\nu)\frac{\partial\chi_3}{\partial z}\right\},$$

$$\sigma_\theta^{(2)}=\frac{E}{1+\nu}\left\{\frac{1}{r}\frac{\partial\chi_1}{\partial r}+\frac{z}{r}\frac{\partial\chi_2}{\partial r}-2\nu\frac{\partial\chi_2}{\partial z}+(1-2\nu)\frac{\partial\chi_3}{\partial z}\right\},$$

(4.2)

$$\sigma_z^{(2)}=\frac{E}{1+\nu}\left\{\frac{\partial^2\chi_1}{\partial z^2}+z\frac{\partial^2\chi_2}{\partial z^2}-2(1-\nu)\frac{\partial\chi_2}{\partial z}-r\frac{\partial^2\chi_3}{\partial r\,\partial z}-2(2-\nu)\frac{\partial\chi_3}{\partial z}\right\},$$

$$\tau_{rz}^{(2)}=\frac{E}{1+\nu}\left\{\frac{\partial^2\chi_1}{\partial r\,\partial z}+z\frac{\partial^2\chi_2}{\partial r\,\partial z}-(1-2\nu)\frac{\partial\chi_2}{\partial r}+r\frac{\partial^2\chi_3}{\partial z^2}-2(1-\nu)\frac{\partial\chi_3}{\partial r}\right\},$$

where $\nabla^2\chi_1=\nabla^2\chi_2=\nabla^2\chi_3=0$.

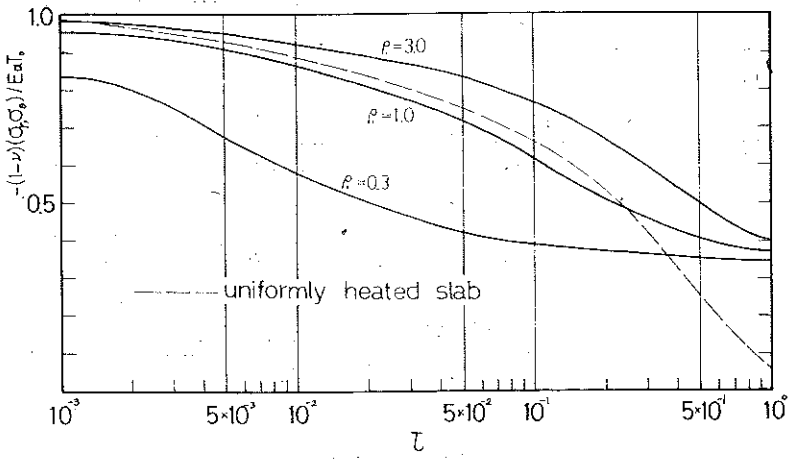

Fig. 4. Maximum compressive stresses as functions of time ($\zeta=\pm1$, $\rho=0$).

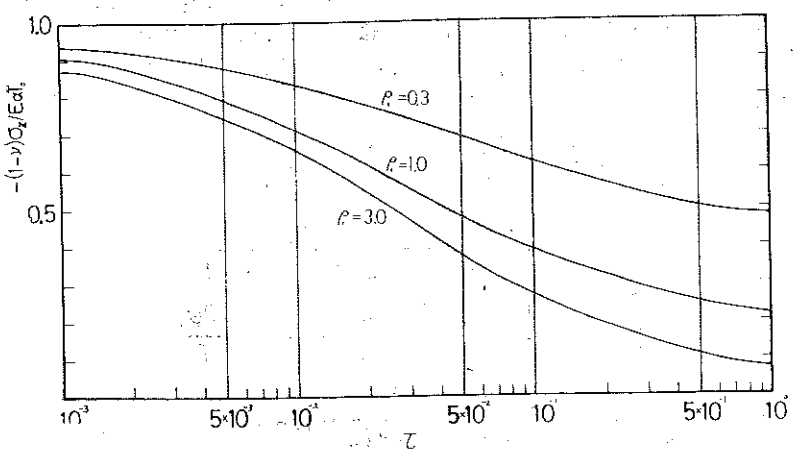

Fig. 5. Maximum axial stresses as functions of time ($\rho=\rho_1$, $\zeta=0$).

The harmonic functions are assumed in the form:

for Case A

$$\frac{1-\nu}{1+\nu}\frac{\psi_1}{\alpha T_0 d^2}=\int_0^\infty \frac{f_0(\xi)}{\xi^2}\operatorname{ch}\xi\zeta J_0(\xi\rho)\,d\xi,$$

$$\frac{1-\nu}{1+\nu}\frac{\psi_2}{\alpha T_0 d}=\int_0^\infty \frac{g_0(\xi)}{\xi}\operatorname{sh}\xi\zeta J_0(\xi\rho)\,d\xi; \tag{4.3}$$

for Case B

$$\frac{1-\nu}{1+\nu}\frac{\chi_1}{\alpha T_0 d^2}=A\rho_1^2\log\rho+\sum_{n=0}^{\infty}\frac{B_n}{\omega_n^2}\frac{K_0(\omega_n\rho)}{K_0(\omega_n\rho_1)}\cos\omega_n\zeta+$$

$$+\int_0^\infty \frac{f_1(\xi)}{\xi^2}\operatorname{ch}\xi\zeta\, C_0(\xi\rho)\,d\xi,$$

$$\frac{1-\nu}{1+\nu}\frac{\chi_2}{\alpha T_0 d}=\int_0^\infty \frac{g_1(\xi)}{\xi}\operatorname{sh}\xi\zeta C_0(\xi\rho)\,d\xi, \tag{4.4}$$

$$\frac{1-\nu}{1+\nu}\frac{\chi_3}{\alpha T_0 d}=\sum_{n=0}^{\infty}\frac{C_n}{\omega_n}\frac{K_0(\omega_n\rho)}{K_0(\omega_n\rho_1)}\sin\omega_n\zeta.$$

The unknown functions $f_0(\xi)$, $g_0(\xi)$, $f_1(\xi)$, $g_1(\xi)$ and coefficient A, B_n, C_n are determined from the following conditions:

for Case A

$$[\sigma_z^{(1)}+\sigma_z^{(2)}]_{\zeta=\pm1}=0,\qquad [\tau_{rz}^{(1)}+\tau_{rz}^{(2)}]_{\zeta=\pm1}=0; \tag{4.5}$$

for Case B (4.5) and

$$[\sigma_r^{(1)}+\sigma_r^{(2)}]_{\rho=\rho_1}=0,\qquad [\tau_{rz}^{(1)}+\tau_{rz}^{(2)}]_{\rho=\rho_1}=0. \tag{4.6}$$

5. Determination of the unknown function and coefficients

For Case A, the unknown functions are determined from (4.5), a pair of simultaneous linear algebraic equations. The solution is given by the forms

$$f_0(\xi)=-(1-\nu)\frac{\rho_1 J_1(\xi\rho_1)}{\operatorname{ch}\xi}+$$

$$+\frac{4\rho_1 J_1(\xi\rho_1)}{(\operatorname{sh}2\xi+2\xi)}\{2(1-\nu)\operatorname{ch}\xi-\xi\operatorname{sh}\xi\}\sum_{n=0}^{\infty}\frac{\xi\omega_n^2\, e^{-\tau(\xi^2+\omega_n^2)}}{(\xi^2+\omega_n^2)^2}, \tag{5.1}$$

$$g_0(\xi)=-\frac{\rho_1 J_1(\xi\rho_1)}{2\operatorname{ch}\xi}+\frac{4\rho_1 J_1(\xi\rho_1)}{(\operatorname{sh}2\xi+2\xi)}\operatorname{ch}\xi\sum_{n=0}^{\infty}\frac{\xi\omega_n^2\, e^{-\tau(\xi^2+\omega_n^2)}}{(\xi^2+\omega_n^2)^2}.$$

For Case B, we obtain the following relation from $(4.5)_1$

$$f_1(\xi)=(2-2\nu-\xi \operatorname{th}\xi)\, g_1(\xi). \tag{5.2}$$

Now for $(4.5)_2$, if the relations

$$\frac{K_1(\omega_n\rho)}{K_0(\omega_n\rho_1)}=\frac{2\omega_n}{\pi}\int_0^\infty \frac{C_1(\xi\rho)}{\xi^2+\omega_n^2}\,d\xi,$$

$$\omega_n\rho_1\frac{K_0(\omega_n\rho)}{K_0(\omega_n\rho_1)}=\frac{2\omega_n}{\pi}\left\{\omega_n\rho_1\frac{K_1(\omega_n\rho_1)}{K_0(\omega_n\rho_1)}-2\right\}\int_0^\infty \frac{C_1(\xi\rho)}{\xi^2+\omega_n^2}\,d\xi+ \tag{5.3}$$

$$+\frac{4\omega_n^3}{\pi}\int_0^\infty \frac{C_1(\xi\rho)}{(\xi^2+\omega_n^2)^2}\,d\xi$$

are used, $g_1(\xi)$ can be expressed with B_n and C_n as follows:

$$g_1(\xi)=\frac{2}{\pi}\sum_{n=0}^{\infty}\frac{(-1)^n \operatorname{ch}\xi}{(\xi^2+\omega_n^2)(\operatorname{sh}2\xi+2\xi)}\left[-\frac{a_n\omega_n^2\rho_1}{\pi}\frac{K_1(\omega_n\rho_1)}{K_0(\omega_n\rho_1)}+\right. \tag{5.4}$$

$$+\frac{2a_n\omega_n\xi^2}{(\xi^2+\omega_n^2)}-\frac{2a_n\omega_n\xi^2 e^{-\tau(\xi^2+\omega_n^2)}}{(\xi^2+\omega_n^2)}+2\omega_n B_n+$$

$$\left.+2\omega_n C_n\left\{4-2\nu-\omega_n\rho_1\frac{K_1(\omega_n\rho_1)}{K_0(\omega_n\rho_1)}-\frac{2\omega_n^2}{\xi^2+\omega_n^2}\right\}\right].$$

The unknown coefficient A, for the sake of convenience, may be written as

$$A=2(1-\nu)\int_0^\infty g_1(\xi)\operatorname{ch}\xi\,\frac{C_1(\xi\rho_1)}{\xi\rho_1}\,d\xi. \tag{5.5}$$

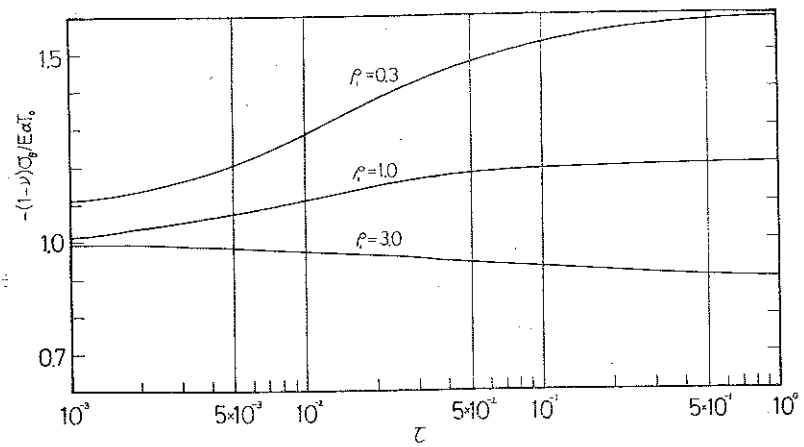

Fig. 6. Maximum circumferential stresses as functions of time ($\rho=\rho_1$, $\zeta=0$).

In (4.6), expanding ch $\xi\zeta$ and $\xi\zeta$ sh $\xi\zeta$ into the Fourier cosin-series, as wen as sh $\xi\zeta$ and $\xi\zeta$ ch $\xi\zeta$ into the sin-series, and equating separately the coefficiellt

each cosin- or sin-function to zero, we obtain a system of linear equations as follows:

$$
\begin{aligned}
&b_n^{(1)} B_n + c_n^{(1)} C_n + \sum_{k=0}^{\infty} \{{}^n b_k^{(1)} B_k + {}^n c_k^{(1)} C_k\} = d_n^{(1)}, \\
&b_n^{(2)} B_n + c_n^{(2)} C_n + \sum_{k=0}^{\infty} \{{}^n b_k^{(2)} B_k + {}^n c_k^{(2)} C_k\} = d_n^{(2)},
\end{aligned} \tag{5.6}
$$

where

$$
b_n^{(1)} = 1 + \frac{K_1(\omega_n \rho_1)}{\omega_n \rho_1 K_0(\omega_n \rho_1)}, \qquad c_n^{(1)} = 1 - 2\nu - \omega_n \rho_1 \frac{K_0(\omega_n \rho_1)}{K_0(\omega_n \rho_1)},
$$

$$
{}^n b_k^{(1)} = -(-1)^{n+k} \frac{16\,\omega_k}{\pi \omega_n \rho_1} \{(1-\nu)\, {}^n\gamma_k^{(1,1)} + \omega_n^2\, {}^n\gamma_k^{(1,2)}\},
$$

$$
\begin{aligned}
{}^n c_k^{(1)} = -(-1)^{n+k} \frac{16\,\omega_k}{\pi \omega_n \rho_1} \Bigg[\left\{ 4 - 2\nu - \omega_k \rho_1 \frac{K_1(\omega_k \rho_1)}{K_0(\omega_k \rho_1)} \right\} \{(1-\nu)\, {}^n\gamma_k^{(1,1)} + \\
+ \omega_n^2\, {}^n\gamma_k^{(1,2)}\} - 2\omega_k^2 \{(1-\nu)\, {}^n\gamma_k^{(2,1)} + \omega_n^2\, {}^n\gamma^{(2,2)}_k\} \Bigg],
\end{aligned}
$$

$$
\begin{aligned}
d_n^{(1)} = -\frac{(-1)^n 8}{\pi \omega_n \rho_1} \sum_{k=0}^{\infty} (-1)^k a_k \omega_k \Bigg[\left\{ \omega_k \rho_1 \frac{K_1(\omega_k \rho_1)}{K_0(\omega_k \rho_1)} - 2 \right\} \{(1-\nu)\, {}^n\gamma_k^{(1,1)} + \\
+ \omega_n^2\, {}^n\gamma_k^{(1,2)}\} + 2\omega_k^2 \{(1-\nu)\, {}^n\gamma_k^{(1,2)} + \omega_n^2\, {}^n\gamma_k^{(2,2)}\} + 2(1-\nu)\, {}^n\delta_k^{(2,1)} + \\
+ 2\omega_n^2\, {}^n\delta_k^{(2,2)} \Bigg] + \frac{a_n}{2} \left\{ 1 + \omega_n \rho_1 \frac{K_1(\omega_n \rho_1)}{K_0(\omega_n \rho_1)} + \frac{4}{\pi \rho_1} I_n \right\},
\end{aligned} \tag{5.7}
$$

$$
b_n^{(2)} = \frac{K_1(\omega_n \rho_1)}{K_0(\omega_n \rho_1)}, \qquad c_n^{(2)} = 2(1-\nu) \frac{K_1(\omega_n \rho_1)}{K_0(\omega_n \rho_1)} - \omega_n \rho_1,
$$

$$
{}^n b_k^{(2)} = -(-1)^{n+k} \frac{16\,\omega_k \omega_n^2}{\pi}\, {}^n\gamma_k^{(1,2)},
$$

$$
{}^n c_k^{(2)} = -(-1)^{n+k} \frac{16\,\omega_k \omega_n^2}{\pi} \left[\left\{ 4 - 2\nu - \omega_k \rho_1 \frac{K_1(\omega_k \rho_1)}{K_0(\omega_k \rho_1)} \right\} {}^n\gamma_k^{(1,2)} - 2\omega_k^2\, {}^n\gamma_k^{(2,2)} \right],
$$

$$
\begin{aligned}
d_n^{(2)} = -\frac{(-1)^n 8\omega_n^2}{\pi} \sum_{k=0}^{\infty} (-1)^k a_k \omega_k \Bigg[\left\{ \omega_k \rho_1 \frac{K_1(\omega) \rho_1)}{K_0(\omega_k \rho_1)} - 2 \right\} {}^n\gamma_k^{(1,2)} + \\
+ 2\omega_k^2\, {}^n\gamma_k^{(2,2)} + 2\, {}^n\delta_k^{(2,2)} \Bigg] + \frac{a_n \omega_n}{2} \left\{ \rho_1 + \frac{4}{\pi} I_n \right\},
\end{aligned}
$$

in which

$$
\begin{aligned}
{}^n\gamma_k^{(i,j)} &= \int_0^{\infty} \frac{\xi\, \mathrm{ch}^2\, \xi\, C_1(\xi \rho_1)}{(\mathrm{sh}\, 2\xi + 2\xi)(\xi^2 + \omega_k^2)^i (\xi^2 + \omega_n^2)^j}\, d\xi, \\
{}^n\delta_k^{(i,j)} &= \int_0^{\infty} \frac{\xi^3\, \mathrm{ch}^2\, \xi\, e^{-\tau(\xi^2 + \omega_n^2)}}{(\mathrm{sh}\, 2\xi + 2\xi)(\xi^2 + \omega_k^2)^i (\xi^2 + \omega_n^2)^j} C_1(\xi \rho_1)\, d\xi, \\
I_n &= \int_0^{\infty} \frac{\xi^2 e^{-\tau(\xi^2 + \omega_n^2)}}{(\xi^2 + \omega_n^2)^2} C_1(\xi \rho_1)\, d\xi.
\end{aligned} \tag{5.8}
$$

6. Numerical calculations and considerations

The value of Poisson's ratio ν was taken as 0.3. Numerical calculations were carried out for three cases of the value ρ_1, namely $\rho_1=0.3$, 1, 3.

For Case A. The graphs for the radial and circumferential stress distributions on the surface, as functions of ρ for various times are shown in Figs. 2 and 3. The curves for σ_θ are discontinuous and have a finite jump at $\rho=\rho_1$, being compared with the continuous curves for σ_r. In a heated region, the maximum compression of σ_θ, as well as σ_r, occurs at the central point of the region as $\tau\to+0$. The maximum tensile circumferential stresses arise in the steady state outside the heated region. In Fig. 4, the effect of the plate thickness to the maximum compressive stresses, which are functions of time, are shown. For the larger value of ρ_1 $(=a/d)$, the thermal stresses decrease to the steady value [2], which is 0.35 in each case, more slowly with respect to time, but the steady thermal stresses of the uniformly heated slab disappear [1].

For Case B. Numerical calculations were carried out for the particular case, which is $a_0=1$, $a_n=0$, $n\geqq 1$, namely cosin-distribution of temperature. The maximum values of σ_z and σ_θ induced on the cylindrical surface, as functions of time, are shown in Figs. 5 and 6. When the value of ρ_1 is small, the remarkable concentration of σ_θ occurs in the steady state, and the steady value for $\rho_1=0.3$ is about -1.6. The axial stresses are large as a value of ρ_1 becomes small and $\tau\to+0$.

7. Conclusion

In the present paper two thermoelastic problems of an infinite slab which is partially exposed to a sudden temperature change, has been analysed and the character of thermal stresses has been clarified by numerical calculations.

(Case A). The maximum compressive stress arises just after temperature change, and the plate thickness greatly affects the decrease of thermal stresses for time.

(Case B). The maximum compressive stress on the cylindrical surface occurs, just after temperature change for the axial stress and in the steady state for the circumferential stress. The stress concentration is remarkable as the plate thickness becomes large.

References

1. M. P. Heisler, J. Appl. Mech., Ser. E., 20, 261, 1953.
2. R. Muki, Trans. Japan Soc. Mech. Engrs., 22, 795, 1956.
3. T. Koizumi, Trans. Japan Soc. Mech. Engrs, 37, 449, 1971.
4. I. N. Sneddon, *Fourier transforms*, p. 159, McGraw-Hill, New York 1951.
5. H. Parkus, *Instationare Warmespannungen*, p. 10. Springer-Verlag, Wien 1959.
6. H. Miyamoto, *Theory of three-dimensional elasticity*, p. 16, Syokabo, Tokyo 1967.

STRESZCZENIE

QUASI-STATYCZNE NAPRĘŻENIA TERMICZNE W NIESKOŃCZONEJ PŁYCIE

W pracy rozważane są dwa zagadnienia termosprężystości: zagadnienie pełnej nieskończonej płyty oraz płyty z otworem cylindrycznym. Rozkład naprężeń termicznych powstałych w płycie wskutek nagłej zmiany temperatury na kołowym obszarze płaskiego brzegu (przypadek A) lub na brzegu cylindrycznym (przypadek B) jest analizowany przy wykorzystaniu potencjału termosprężystego i funkcji naprężenia. W obydwu przypadkach zbadano i pokazano graficznie jak stosunek promienia ogrzanego obszaru kołowego lub otworu cylindrycznego do grubości płyty wpływa na rozkład naprężeń termicznych.

Резюме

КВАЗИСТАТИЧЕСКИЕ ТЕРМИЧЕСКИЕ НАПРЯЖЕНИЯ В БЕСКОНЕЧНОЙ ПЛИТЕ

В работе рассмотрены две задачи термоупрогости: задача полной бесконечной плиты и задача плиты с цилиндрическим отверстием. Распределение термических напряжений, возникнувших в плите вследствие внезанного изменения температуры в круговой области плоской границы (случай А) или на цилиндрической границе (случай Б), анализируется при использовании термоупругого потенцала и функций напряжения. В обоих случаях исследовано и графически представлено как отношение радиуса нагретой круговой области или цилиндрического отверстия к толщине плиты влияет на распределение термических напряжений.

MECHANICAL ENGINEERING II,
TOHOKU UNIVERSITY, SENDAI, JAPAN

Received May 28, 1974 r.